THE JOURNAL OF BIOLOGICAL CHEMISTRY

Vol. 268, No. 32, Issue of November 15, pp. 24022-24031, 1993
Printed in U.S.A.

Study of the Conformation of DARPP-32, a Dopamine- and cAMP-regulated Phosphoprotein, by Fluorescence Spectroscopy*

(Received for publication, May 13, 1993, and in revised form, July 16, 1993)

Paolo Neyroz‡§, Frédéric Desdouits¶‖, Fabio Benfenati, Jay R. Knutson‡‡, Paul Greengard§§, and Jean-Antoine Girault¶**

*From the ‡Dipartimento di Biochimica "G. Moruzzi," Università di Bologna, Bologna, Italy, the ¶Institut National de la Santé et de la Recherche Médicale U 114, Chaire de Neuropharmacologie, Collège de France, Paris, France, the **Dipartimento di Medicina Sperimentale e Scienze Biochimiche, Università di Roma "Tor Vergata," Roma, Italy, the ‡‡Laboratory of Cell Biology, National Heart, Lung, and Blood Institute, National Institutes of Health, Bethesda, Maryland 20892, and the §§Laboratory of Molecular and Cellular Neuroscience, The Rockefeller University, New York 10021*

DARPP-32 is a potent inhibitor of protein phosphatase 1 when it is phosphorylated on Thr^{34} by cAMP-dependent protein kinase. DARPP-32 is also phosphorylated on Ser^{45} and Ser^{102} by casein kinase II, resulting in a facilitation of phosphorylation by cAMP-dependent protein kinase. We have studied the conformation of recombinant rat DARPP-32 by steady-state and time-resolved fluorescence. The steady-state emission spectra and quenching of the intrinsic (Trp^{163}) and extrinsic fluorescence (acrylodan or lucifer yellow linked to Cys^{72}) were consistent with a complete exposure of these residues to the aqueous environment. The intrinsic fluorescence of DARPP-32 was resolved into three decay components with lifetimes of 1, 3.4, and 7 ns, with the intermediate lifetime component giving the major contribution. The ratio between the amplitudes associated with the short and long decay constants was decreased upon denaturation. The rotational behavior of DARPP-32 measured by anisotropy decay revealed that Trp^{163} is located in a highly flexible peptide chain, whereas Cys^{72} is embedded in a more rigid environment. Phosphorylation by cAMP-dependent protein kinase did not alter any of the fluorescence parameters, whereas only minor effects were associated with casein kinase II phosphorylation. These findings indicate that DARPP-32 contains at least two distinct domains and that phosphorylation has no dramatic effects on its conformation.

Like protein kinases, protein phosphatases play an important role in signal transduction pathways, but the mechanisms of their regulation are not as well characterized. Phosphoserine/phosphothreonine phosphatases have been classified by Ingebritsen and Cohen (1983) into two types, 1 and 2, according to their substrate preference and their inhibition by heat stable inhibitors. Type 1 phosphatases preferentially dephosphorylate the β-subunit of phosphorylase kinase and are inhibited by phosphoinhibitor-1 and inhibitor-2. Inhibitor-1 is a heat-stable protein which has a relatively wide tissue distribution (Hemmings *et al.*, 1992). Another phosphatase 1 inhibitor called DARPP-32[1] (*d*opamine- and c*A*MP-*r*egulated *p*hospho*p*rotein with an apparent M_r of 32,000 on SDS-polyacrylamide gel electrophoresis) is expressed in some specific cell types, including neurons which possess the D1 type of dopamine receptor (Hemmings *et al.*, 1987). Inhibitor-1 and DARPP-32, which are encoded by distinct genes, have an overall amino acid sequence identity of ~25% (Williams *et al.*, 1986). They are both phosphorylated by cAMP-dependent protein kinase (PKA) on a threonine residue at position 34 in DARPP-32 and at position 35 in inhibitor-1 (Hemmings *et al.*, 1984d; Aitken *et al.*, 1982). The amino acid sequences surrounding these threonines are highly conserved between the two proteins (Aitken *et al.*, 1982; Williams *et al.*, 1986). When DARPP-32 or inhibitor-1 are phosphorylated by PKA, they are very potent inhibitors of phosphatase 1 catalytic subunit (PP1c, $IC_{50} < 1$ nM), whereas the nonphosphorylated forms are inactive (Hemmings *et al.*, 1984a; Huang and Ginsburg, 1976). In both inhibitor-1 and DARPP-32, the threonine involved in PP1c inhibition is also phosphorylated by cGMP-dependent protein kinase and is dephosphorylated by phosphatase 2A and phosphatase 2B (calcineurin), *in vitro* as well as in intact cells (King *et al.*, 1984; Halpain *et al.*, 1990). Thus, these two inhibitors provide a means by which extracellular signals acting through cAMP, cGMP, or Ca^{2+} can modulate the activity of protein phosphatase 1. The phosphatase inhibition appears to be of a mixed mechanism, competitive and noncompetitive, and is reproduced by a relatively short peptide surrounding the phosphorylation site (from residue 9 to 38; see Hemmings *et al.*, (1990)).

Efforts have been made to elucidate the biochemical differences between DARPP-32 and inhibitor-1 under the assumption that the function of these two proteins may be complementary rather than redundant. Although the sequences of the COOH-terminal halves of DARPP-32 and inhibitor-1 are different, they are each highly conserved among various mammalian species, suggesting that they have an important role (Aitken *et al.*, 1982; Elbrecht *et al.*, 1990; Williams *et al.*, 1986;

* This work was supported by grants from the Institut National de la Santé et de la Recherche Médicale, the National Alliance for the Mentally Ill (Stanley Award), National Parkinson Foundation (to J.-A. G.), and the Italian Consiglio Nazionale delle Ricerche (to F. B.), a Consiglio Nazionale delle Ricerche/Institut National de la Santé et de la Recherche Médicale collaborative grant (to F. B. and J.-A. G.), and a NATO collaborative grant (to F. B., P. N., and P. G.) The costs of publication of this article were defrayed in part by the payment of page charges. This article must therefore be hereby marked "*advertisement*" in accordance with 18 U.S.C. Section 1734 solely to indicate this fact.

§ To whom correspondence should be addressed: Dipartimento di Biochimica "G. Moruzzi" (Sezione de Biochimica Farmaceutica), Via San Donato 19/2, 40126 Bologna, Italy. Tel.: 39-51-25318; Fax: 39-51-242978.

‖ Supported by fellowships from DRET and Rhône-Poulenc Rorer.

[1] The abbreviations used are: DARPP-32, dopamine- and cAMP-regulated phosphoprotein with apparent M_r of 32,000; CKII, casein kinase II; DAS, decay-associated spectra; PKA, cyclic AMP-dependent protein kinase; PP1c, protein phosphatase 1 catalytic subunit.

Kurihara *et al.*, 1988; Ehrlich *et al.*, 1990). The DARPP-32 sequence includes an unusual stretch of 18 acidic residues starting at position 119 in the rat, which is not present in inhibitor-1 (Ehrlich *et al.*, 1990). In addition, casein kinase II (CKII) phosphorylates DARPP-32 on Ser^{45} and Ser^{102}, both *in vitro* and *in vivo*, but does not phosphorylate inhibitor-1 (Girault *et al.*, 1989) (see Fig. 1). Phosphorylation of DARPP-32 by CKII does not directly affect its ability to inhibit phosphatase 1, but facilitates its phosphorylation by PKA (Girault *et al.*, 1989).

The present study was undertaken to determine whether the marked changes in the functional properties of DARPP-32 observed after phosphorylation by PKA and CKII are associated with conformational changes of the protein in solution. Using recombinant rat DARPP-32 expressed in *Escherichia coli* and phosphorylated *in vitro* by purified PKA or CKII, we have studied the steady-state and time-resolved fluorescence of the single tryptophan residue (Trp^{163}) present in the COOH-terminal region and of fluorescent probes covalently linked to the single cysteine residue (Cys^{72}) present in the NH_2-terminal region of the molecule. The results obtained on the photophysical properties and the rotational relaxation kinetics of DARPP-32 provide information on the microenvironment of the tryptophan and cysteine residues and give insights on the possible occurrence of long-range conformational transitions in response to site-specific phosphorylation.

EXPERIMENTAL PROCEDURES

Materials

Rat DARPP-32 cDNA in pGEM was provided by Dr. Michelle Ehrlich (The Rockefeller University). pET-3a plasmid and HMS174 and BL21 (DE3) *E. coli* strains were a gift of Dr. William Studier (Brookhaven National Laboratory). Lucifer yellow-iodoacetamide and acrylodan were from Molecular Probes. PKA catalytic subunit and CKII were purified from bovine heart (Kaczmarek *et al.*, 1980) and from calf thymus (Hathaway and Traugh, 1983), respectively. DE52 was from Whatman, Dowex AG 1X8 from Bio-Rad, Sephadex G-100 from Pharmacia LKB Biotechnology Inc., Aquapore Octyl column from Applied Biosystems, Aquacid II from Calbiochem, and [γ-^{32}P]ATP from Du Pont-New England Nuclear.

Production and Purification of Recombinant Rat DARPP-32

A rat DARPP-32 cDNA clone placed in a M13 phage was polymerase chain reaction-amplified using primers corresponding to the 5′ and 3′ ends of the coding sequence plus additional nucleotides providing the appropriate restriction sites for inclusion in pET-3a, a bacterial vector allowing expression of high levels of native (*i.e.* nonfusion) recombinant proteins (Rosenberg *et al.*, 1987). The amplified DNA was cut with *Nde*I and *Bam*HI and inserted into pET-3a expression vector, under the dependence of a ϕ10 promoter for T7 polymerase (Rosenberg *et al.*, 1987). The absence of cloning or polymerase chain reaction artifacts was verified by complete nucleotide sequencing of the coding sequence of the DARPP-32 construct.

E. coli BL21 (DE3) were transformed with recombinant pET-3a plasmids coding for DARPP-32. This lysogenic strain expresses T7 polymerase under control of a *lac* repressor, allowing the induction of the recombinant protein by IPTG (Rosenberg *et al.*, 1987). Bacteria were grown in 20 l high-density cultures, in the presence of ampicillin, at Pasteur Institute Fermentation Facility (Paris). After isopropyl-1-thio-β-D-galactopyranoside induction, bacteria were collected by centrifugation, frozen in liquid nitrogen, and kept at −80 °C. Bacteria (~600 g) were homogenized with an Ultraturrax in 2 liters of buffer containing 50 mM Tris, pH 8, 5 mM EDTA, 0.1 mM phenylmethylsulfonic acid, 15 mM β-mercaptoethanol, and 0.5 g/liter lysozyme, at 4 °C. The homogenate was centrifuged at 25,000 × *g* for 45 min. The pH of the supernatant was brought to 2 with H_2SO_4 while the temperature was maintained at 4 °C. After Ultraturrax homogenization the acid insoluble material was eliminated by centrifugation at 16,000 × *g* for 30 min and the pH of the supernatant was neutralized with NH_3. The solution was then heated to 100 °C for 2 min, cooled to room temperature on ice, and centrifuged at 16,000 × *g* for 30 min. The soluble proteins were batch-adsorbed on 300 ml of DE52 anion-exchange resin. After washing with 3 liters of 10 mM triethanolamine-Cl, pH 7.5, 2 mM EDTA, 1 mM EGTA, 0.1 mM phenylmethylsulfonyl fluoride, and 15 mM β-mercaptoethanol, the resin was poured in a column, and developed in the same buffer with a 1-liter gradient of 0–1 M NaCl. The peak fractions were dialyzed against 10 mM Hepes, pH 7.4, 2 mM EDTA, 1 mM EGTA, 0.1 mM phenylmethylsulfonyl fluoride, and 15 mM β-mercaptoethanol. At this stage, the purified DARPP-32 was virtually devoid of other protein contaminants, but contained 2 proteins of smaller size, which were immunoreactive with anti-DARPP-32 antibodies, and which probably corresponded to proteolytic fragments or to incomplete synthesis. Further purification of DARPP-32 was achieved by gel filtration on a Sephadex G-100 column (94 × 1.6 cm) and by reverse-phase high performance liquid chromatography on an Aquapore Octyl column (25 × 1 cm) eluted with increasing concentrations of acetonitrile in water, in the presence of 0.1% trifluoroacetic acid. Fractions containing DARPP-32 were lyophilized in a Speedvac concentrator and resuspended in water with 1 mM β-mercaptoethanol. The purity of the DARPP-32 preparations was analyzed by SDS-polyacrylamide gel electrophoresis (Laemmli, 1970) followed by staining the gels with Coomassie Brilliant Blue. Protein concentration was determined by amino acid composition and by a bicinchoninic acid-based method (Smith *et al.*, 1985) using bovine serum albumin as a standard. The latter method underestimated the protein concentration by a factor of ~0.75 as compared to amino acid composition. The properties of recombinant rat DARPP-32 were identical to those of the protein purified from rat brain: it had an apparent M_r of ~34,000 on SDS-polyacrylamide gel electrophoresis and an exclusion volume on gel filtration corresponding to an apparent M_r of ~55,000.[2] These values, which are surprising for a protein whose predicted M_r is ~22,000, are similar to those observed for bovine DARPP-32 (Hemmings *et al.*, 1984b), and are attributable to the poor binding of SDS and to the elongated shape of the molecule.

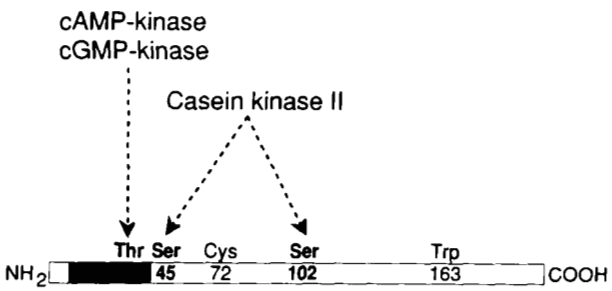

FIG. 1. **Structural model of DARPP-32.** The primary structure of rat DARPP-32 (total length, 205 amino acids) is schematically depicted with the locations of Thr^{34} phosphorylated by cAMP-dependent protein kinase and cGMP-dependent protein kinase and of the two serine residues (Ser^{45} and Ser^{102}) phosphorylated by casein kinase II. The single tryptophan residue (Trp^{163}) used in the intrinsic fluorescence measurements and the single cysteine residue (Cys^{72}) used to conjugate DARPP-32 with thiol-reactive extrinsic fluorophores are also shown. The *hatched* area corresponds to the minimal sequence required for phosphatase inhibition (Hemmings *et al.*, 1990).

Phosphorylation of DARPP-32

Phosphorylation by PKA was carried out in a buffer containing 50 mM Hepes, pH 7.4, 1 mM EGTA, 10 mM magnesium acetate, 2 mM ATP, and PKA catalytic subunit for 1 h at 30 °C. Phosphorylation by CKII was carried out in a buffer containing 50 mM Tris-Cl, pH 7.4, 150 mM KCl, 20 mM magnesium acetate, 2 mM ATP, and CKII for 3 h at 30 °C. Reactions were stopped by the addition of trichloroacetic acid to a final concentration of 10% (w/v), and incubation on ice for 15 min. Proteins were collected by centrifugation, resuspended in 10 mM Hepes, pH 7.4, 1 mM EDTA, and 1 mM β-mercaptoethanol, and dialyzed extensively against the same buffer. In some experiments reactions were stopped by the addition of acetic acid to a final concentration of 30% (v/v), ATP was removed by chromatography on a Dowex AG X8 column, and DARPP-32 was further purified by high performance liquid chromatography on Aqua-

[2] F. Desdouits and J.-A. Girault, unpublished observations.

pore Octyl, as described above. A trace amount of [γ-^{32}P]ATP was added to the reaction mixtures for determining the stoichiometry of phosphorylation, which averaged 1 mol of phosphate/mol of protein for PKA and was ≥2 for CKII. The kinetics of phosphorylation of recombinant rat DARPP-32 and its phosphorylated sites, studied by two-dimensional thermolytic phosphopeptide mapping, were identical to those previously identified in rat DARPP-32 (Hemmings *et al.*, 1984c; Girault *et al.*, 1989). Nonspecific phosphorylation at sites other than the specific ones was less than 10%. Nonphosphorylated DARPP-32 was subjected to the same precipitation and purification steps as phosphorylated samples. In addition, recombinant DARPP-32 phosphorylated by PKA inhibited phosphatase 1 with an IC_{50} ~ 0.5 nM.[2]

Conjugation of Thiol-specific Fluorophores to DARPP-32

DARPP-32 was dialyzed against 10 mM Hepes, pH 7.4, 1 mM EDTA, in the presence of 1 mM β-mercaptoethanol and then in the absence of β-mercaptoethanol and under nitrogen bubbling in order to prevent oxidation of the sulfhydryl groups. DARPP-32 was then incubated in the presence of a 10-fold molar excess of acrylodan (Prendergast *et al.*, 1983) or lucifer yellow/iodoacetamide (Haugland, 1992) for 12 h at 4 °C in the dark. The unconjugated fluorophore was removed by sedimentation and by subjecting the soluble fraction to extensive dialysis against 10 mM Hepes, pH 7.4, 1 mM EDTA, followed by gel filtration on a Superfine G-25 Sephadex column (1.2 × 7 cm) equilibrated in the same buffer. The incorporation of the thiol-specific fluorescent probes into DARPP-32 was checked by illuminating the unfixed gels with UV light. The fluorophore/protein molar ratios, calculated according to the reported molar extinction coefficients for the fluorophores and to the experimentally determined extinction coefficient for rat DARPP-32 ($E^{1\%}_{280}$ = 3.50), ranged from 0.8 to 1.

Circular Dichroism

Circular dichroism spectra were recorded on a Jasco 500A spectropolarimeter equipped with a computer for data accumulation. Protein samples (0.2 mg/ml) in 10 mM Hepes, pH 7.4, 1 mM EDTA were measured in a 0.2-mm path length cell. Typically 4–8 spectra were accumulated and averaged to achieve appropriate signal-to-noise ratios. The fractional composition of the secondary structure of DARPP-32 in terms of α-helix and random coil was evaluated as described by Greenfield and Fassman (1969).

Fluorescence Spectroscopy Measurements

Technical steady-state fluorescence excitation and emission spectra were obtained with Perkin-Elmer MPF-44A and LS-50 spectrofluorometers using excitation and emission band widths of 5 nm each. The steady-state emission anisotropy was determined using either a Polacoat dichroic polarizer (Ealing Electroptics, United Kingdom) or a linear polarizer Polaroid HNP'B (Polaroid Corp., Cambridge, MA) installed in the excitation path and a Polaroid HNP'B filter in the emission path. The relative intensities for the four combinations of vertically (v) and horizontally (h) polarized beams (I_{vv}, I_{vh}, I_{hh}, I_{hv}) were recorded in the "ratio mode."

Steady-state emission anisotropy was calculated as follows:

$$\langle r \rangle = \frac{GI_{vv} - I_{vh}}{GI_{vv} + 2I_{vh}} \quad \text{(Eq. 1)}$$

where $G = I_{hh}/I_{hv}$ is the grating correction factor introduced to normalize for the different sensitivity of the system to detect the horizontally and vertically polarized emission (Azumi and McGynn, 1962; Paoletti and LePecq, 1969).

Fluorescence quenching of DARPP-32 was carried out using acrylamide and potassium iodide as quenchers. Protein samples at increasing concentrations of the quencher were prepared by adding small aliquots from concentrated solutions (acrylamide, 8 M; KI, 4 M). When required, corrections were introduced according to Parker (1968). The steady-state fluorescence data were analyzed according to the Stern-Volmer equation (Birks, 1970):

$$F_o/F = 1 + K_{sv}[Q] = \tau_0/\tau \quad \text{(Eq. 2)}$$

where F_o and F are the fluorescence intensities measured in the absence and the presence of the quencher, K_{sv} is the Stern-Volmer constant, and [Q] is the quencher concentration. K_{sv} is related to the bimolecular quenching constant (k_q) and to the mean fluorescence lifetime in the absence of quencher (τ_0) as follows:

$$K_{sv} = k_q \cdot \tau_0 \quad \text{(Eq. 3)}$$

where k_q represents a measure of the accessibility of the fluorophore to the external environment.

Nanosecond time-resolved fluorescence measurements were obtained using a time-correlated single photon counting apparatus (Ware, 1972, Yguerabide, 1972; O'Connor and Philips, 1984) equipped with either a laser source (Model 2040/3500, Spectra-Physics, CA) or with a thyratron-gated nitrogen flash lamp (model F199, Edinburgh Instruments, United Kingdom) as exciting source and with the typical NIM electronic modules (EG&G Ortec, TN). The decay of the total fluorescence intensity was recorded under "magic angle" conditions (Badea and Brand, 1979) and the wavelength-dependent time shift of the photomultiplier (Wahl *et al.*, 1974) was determined in a separate experiment using melatonin as a standard. Experimental curves, collected to resolve the spectra associated with the individual decay constants (decay-associated spectra, DAS) (Knutson *et al.*, 1982), were obtained by stepping the emission monochromator in increments of 5 nm between 300 and 450 nm.

The decay of the emission anisotropy of DARPP-32 and of lucifer yellow-DARPP-32 was measured as previously described (Dale *et al.*, 1977), using a combination of two Polacoat dichroic polarizers parallel (vv) and crossed (vh) with respect to the excitation and the emission paths. A depolarizer DPU-15 (Optics for Research, NJ) placed in front of the emission monochromator slit was used to eliminate for "G-factor" corrections ($G \approx 1.00$). Decay curves for the polarized components of the emitted fluorescence were separately collected within the same experimental time course by alternative collection of equal timed curves for "lamp," "I_{vv}," and "I_{vh}," the latter pair obtained by automated rotation of a film polarizer.

Fluorescence Data Analysis

Fluorescence Intensity Decay—The decay data were analyzed by the nonlinear least square method (Bevington, 1969; Knight and Selinger, 1971; Grinvald and Steinberg, 1974), and decay curves collected at multiple emission wavelengths were simultaneously analyzed according to the global procedure described by Knutson *et al.* (1983). The experimental data were analyzed assuming that the fluorescence decay follows a multiexponential law:

$$I(t) = \Sigma\ \alpha_i \cdot e^{-t/\tau_i} \quad \text{(Eq. 4)}$$

where the relative amplitudes, α_i, and the decay constants, τ_i are the numerical parameters to be recovered. The best fit between the theoretical curve and the data was evaluated from the plot of residuals, the autocorrelation function of the residuals, and the reduced Chi-square (χ^2) (Bevington, 1969). The DAS were obtained by the global procedure (Beechem *et al.*, 1985) and the fluorescence relative intensities at the various wavelengths were expressed as $\alpha_i \cdot \tau_i$ products.

Fluorescence Anisotropy Decay—The anisotropy decay can be described by a sum of discrete exponential terms as follows (Wahl, 1969;Tao, 1969):

$$r(t) = \Sigma\ \beta_i \cdot e^{-t/\phi_i} \quad \text{(Eq. 5)}$$

where the sum of the pre-exponential terms, β_i, is the anisotropy in the absence of rotation, r_o, and the ϕ_i values are the rotational correlation times. The parameters for the decay of anisotropy, $r(t)$, were recovered from the analysis of the experimental decays of the polarization components, $I_{vv}(t)$, and, $I_{vh}(t)$, by either the *sum and difference* approach of Dale *et al.* (1977) or the *system analysis* approach introduced by Gilbert (1983). According to this method, the fitting functions to obtain $r(t)$ are the following (Ameloot *et al.*, 1984; Cross and Fleming, 1984).

$$I_{vv}(t) = 1/3\ s(t) \cdot (1 + 2r(t)) \quad \text{(Eq. 6)}$$

$$I_{vh}(t) = 1/3\ s(t) \cdot (1 - r(t)) \quad \text{(Eq. 7)}$$

Unless otherwise stated, all the fluorescence experiments were carried out at 22 °C. The variability of the decay parameters was evaluated by determining the joint confidence intervals (Johnson, 1983). All the steady-state and time-resolved fluorescence experiments were run at least twice using different preparations of DARPP-32 phosphorylated and/or labeled with extrinsic fluorescent probes. The inter-experimental variability was less than 10%.

RESULTS

Circular Dichroism—The substantial heat stability and the peculiar hydrodynamic properties of DARPP-32 (Hemmings *et al.*, 1984b) suggest that it has an elongated shape and an unfolded tertiary structure. Indeed, the CD spectrum of recombinant rat DARPP-32 (Fig. 2) indicates that very little organization is present in the secondary structure of the protein (less than 10% α-helix, as calculated by the method of Greenfield and Fassman (1969)) and that most of the protein structure consists of a random coil. The CD spectrum of bovine DARPP-32 purified from brain as described by Hemmings *et al.* (1984b) closely resembled that of recombinant DARPP-32 (data not shown), suggesting that the expression of the protein in *E. coli* did not alter its molecular structure.

Steady-state Fluorescence—The steady-state emission spectra of intrinsic and extrinsic fluorescence of native and denatured DARPP-32 are presented in Fig. 3. Under native conditions, the maximum of the tryptophan emission intensity was centered at 352 nm, as expected for partially unfolded proteins. When DARPP-32 was subjected to denaturation in 8 M urea, the tryptophan emission spectrum was not shifted but its intensity was increased by approximately 15–20%, probably due to the removal of a quenching mechanism present in the native protein (Fig. 3, *upper panel*).

In agreement with the results of the intrinsic fluorescence, the spectral distribution of the fluorescence of acrylodan and lucifer yellow conjugated to DARPP-32 did not change appreciably upon denaturation of the protein (Fig. 3, *middle* and *lower panels*). In particular, the emission spectrum of DARPP-32 conjugated to acrylodan, a reagent very sensitive to solvent polarity (Prendergast *et al.*, 1983), exhibited a λ_{max} at 513 nm, very similar to that observed for the β-mercaptoethanol adduct (λ_{max} at 520 nm). This observation, together with the absence of noticeable spectral changes upon denaturation (λ_{max} at 516 nm), demonstrates that the cysteine residue in the NH_2-terminal part of DARPP-32 is fully exposed to the aqueous environment. Moreover, no detectable spectral shifts of either the intrinsic or the extrinsic fluorescence were observed at various ionic strengths (0–250 mM NaCl) or when DARPP-32 was phosphorylated by either PKA or CKII (not shown).

To assess if peptide regions surrounding the tryptophan and the cysteine residues (see Fig. 1) could be distinguished by different accessibility to small molecules, quenching measurements of the intrinsic and the extrinsic fluorescence of DARPP-32 were carried out. Acrylamide, a polar and uncharged compound, and iodide, a negatively charged ion, were used as quenchers. The Stern-Volmer plots obtained from these experiments are shown in Fig. 4. The K_{sv} values and the corresponding quenching rate constants k_q relative to the two fluorophores did not significantly change upon phosphorylation and were in the order of magnitude of the values reported

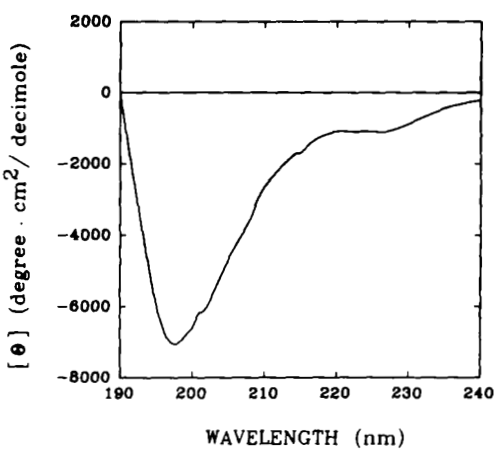

FIG. 2. **Circular dichroic spectrum of DARPP-32.** CD spectrum of recombinant nonphosphorylated rat DARPP-32 was obtained at a protein concentration of 0.25 mg/ml in 10 mM Hepes, pH 7.4, and 1 mM EDTA. Data are plotted as molar ellipticity, [θ], *versus* wavelength (nm).

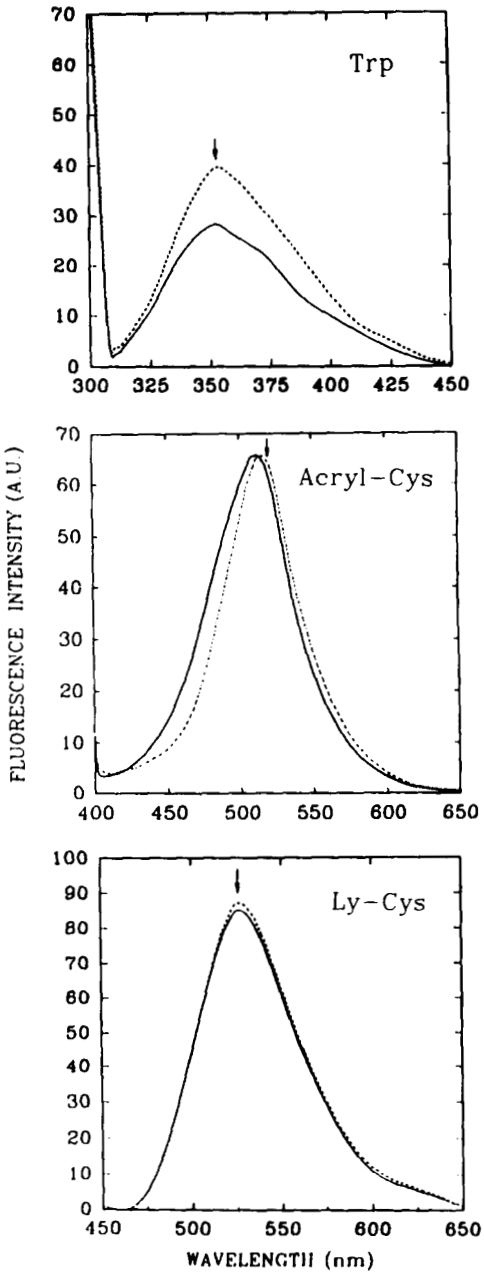

FIG. 3. **Steady-state emission spectra of intrinsic and extrinsic fluorescence of DARPP-32.** Native DARPP-32 (0.2 mg/ml, *upper panel*), DARPP-32 conjugated to acrylodan (0.1 mg/ml, *middle panel*), and DARPP-32 conjugated to lucifer yellow (*Ly*) (0.1 mg/ml, *lower panel*) were dissolved in 10 mM Hepes, pH 7.4), 1 mM EDTA in the absence (*solid line*) or presence of 8 M urea (*dashed line*). Samples were excited at 295 (tryptophan), 391 (acrylodan), and 430 (lucifer yellow) nm and the relative fluorescence intensities are reported in arbitrary units. *Arrows* indicate the position of the emission peaks of the fluorophores fully exposed to aqueous environment (melatonin and the 2-mercaptoethanol adducts of acrylodan and lucifer yellow for the *upper*, *middle*, and *lower panels*, respectively).

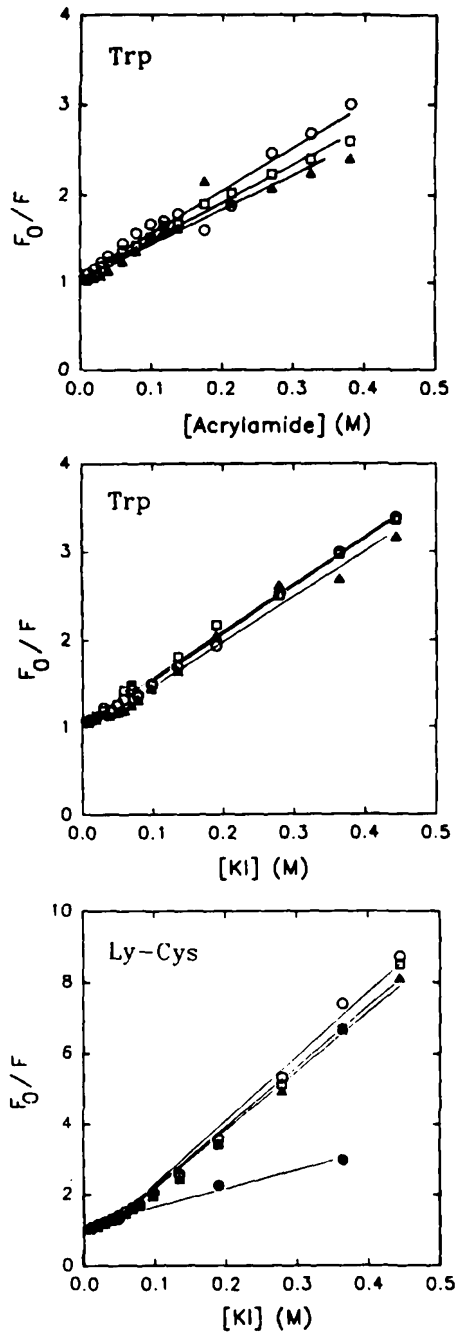

FIG. 4. **Stern-Volmer plots of DARPP-32 intrinsic and extrinsic fluorescence quenching in various phosphorylation states.** In the *upper* and *middle panels*, the quenching data of the intrinsic fluorescence of nonphosphorylated (○), PKA-phosphorylated (□), and CKII-phosphorylated (▲) DARPP-32 using acrylamide or potassium iodide are reported. Excitation and emission wavelengths of 295 and 350 nm were used, respectively. DARPP-32 (0.2 mg/ml) was dissolved in 10 mM Hepes, pH 7.4, 1 mM EDTA, in the absence or presence of various concentrations of the quencher. The data were fitted using linear regression according to Equation 2. The points represent the means of three separate experiments. The bimolecular rate quenching constants (k_q) for the nonphosphorylated, PKA-phosphorylated, and CKII-phosphorylated forms of DARPP-32 were: 1.35, 1.18, and 1.11 10^9 M^{-1} s^{-1} for the acrylamide quenching; 1.52, 1.51, and 1.45 10^9 M^{-1} s^{-1} for the KI quenching. In the *lower panel* the quenching data of the extrinsic fluorescence of the different forms of DARPP-32 conjugated with lucifer yellow (*Ly*) using KI, are shown. The upward curvatures of the Stern-Volmer graphs are suggestive of a mixed static and collisional quenching mechanism. The *filled circles* are the data obtained by time-resolved measurements at four increasing concentrations of KI. These data are plotted as, $\langle\tau_0\rangle/\langle\tau\rangle$, and were used to calculate the k_q for the purely collisional quenching of lucifer yellow-labeled DARPP-32. The values for the nonphosphorylated, PKA-phosphorylated, and CKII-phosphorylated forms did not significantly differ (k_q, 0.99 10^9 M^{-1} s^{-1}). The fluorescence decay of lucifer yellow-labeled DARPP-32, measured in the absence of the quencher, was best described by a double exponential function with the following decay parameters: $\alpha_1 = 0.27$, $\tau_1 = 3.05$ ns, $\alpha_2 = 0.73$, $\tau_2 = 8.48$ ns. No significant quenching of lucifer yellow fluorescence was detected using acrylamide as a quencher.

TABLE I

Steady-state fluorescence anisotropy of DARPP-32

The steady-state emission anisotropy was determined using linear polarizer filters (Polaroid HNP'B) installed in the excitation and emission paths. The relative intensities for the four combinations of vertically and horizontally polarized beams were recorded in the ratio mode and the steady-state emission anisotropy was calculated as described under "Experimental Procedures" for both the intrinsic fluorescence ($\langle r\rangle$Trp) and the extrinsic fluorescence of lucifer yellow (Ly)-conjugated DARPP-32 ($\langle r\rangle$Ly). Excitation and emission wavelength were 295 and 350 nm (tryptophan fluorescence) or 430 and 530 nm (lucifer yellow fluorescence), respectively. Steady-state emission anisotropy determined on acrylodan-labeled DARPP-32 yielded values in the same range as those obtained with lucifer yellow DARPP-32 (not shown). Data are means ±S.E. of at least six different measurements.

DARPP-32	$\langle r\rangle$Trp	$\langle r\rangle$Ly
Nonphosphorylated	0.040 ± 0.006	0.097 ± 0.008
PKA phosphorylated	0.048 ± 0.005	0.100 ± 0.007
CKII phosphorylated	0.054 ± 0.006	0.094 ± 0.008
Nonphosphorylated, 8 M urea	0.016 ± 0.010	0.062 ± 0.008

for proteins containing exposed fluorophores (Eftink and Ghiron, 1976). Lucifer yellow was totally refractory to acrylamide quenching (not shown), and therefore no information about accessibility could be obtained using this fluorophore-quencher pair.

In order to investigate whether site-specific phosphorylation induces changes in DARPP-32 structure detectable by steady-state techniques, measurements of the time-averaged fluorescence anisotropy, $\langle r\rangle$, of Trp^{163} and of lucifer yellow-Cys^{72} were carried out (Table I). The relatively low values found for the fluorescence anisotropy of Trp^{163} indicate that the peptide chain surrounding this residue is characterized by independent segmental motions which are little changed by site-specific phosphorylation. The higher anisotropy values obtained for the lucifer yellow emission suggest that the cysteine residue resides in a region of the protein with relatively constrained rotational flexibility. In view of previous results (Hemmings *et al.*, 1984b), these $\langle r\rangle$ values are compatible with the overall rotational movements of much of the protein. The lack of a significant effect of site-specific phosphorylation also suggests that this DARPP-32 domain does not undergo large structural changes. Urea (8 M) denaturation of DARPP-32 substantially reduced the $\langle r\rangle$ values for both fluorophores, suggesting that under denaturing conditions DARPP-32 can be further unfolded.

Time-resolved Fluorescence—Time-resolved studies on the intrinsic fluorescence of DARPP-32 were carried out under various experimental conditions. Fig. 5 shows a typical fluorescence decay curve of DARPP-32 which was fitted to a mono- or multiexponential decay model. The statistical analysis of the goodness of fit clearly demonstrated that, in spite of the presence of a single tryptophan residue, the fluorescence intensity decay was best described by the sum of three discrete components with lifetimes of approximately 1, 3.4, and 7.3 ns (Table II). The three lifetimes were not significantly affected by ionic strength (not shown), or site-specific phosphorylation.

In order to uncover possible conformational changes of

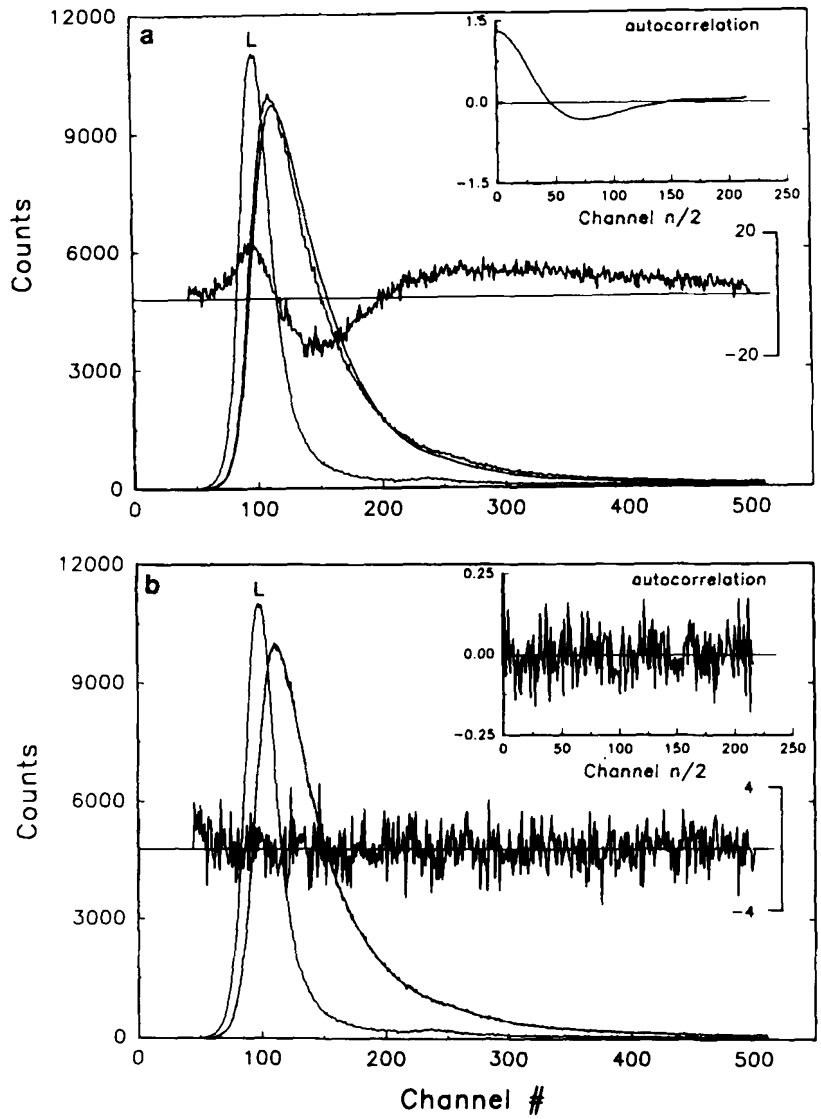

FIG. 5. **Analysis of the fluorescence intensity decay of DARPP-32.** Fluorescence decay data were obtained at 22 °C using an excitation wavelength of 295 nm (band pass 4 nm) and the fluorescence emission was observed at 350 nm (band pass 10 nm). The protein concentration was 0.2 mg/ml in a buffer containing 10 mM Hepes, pH 7.4, and 1 mM EDTA. The calibration time for each channel was 0.0862 ns. Photon counts are reported on the *y* axis in a linear scale. The excitation lamp profile is indicated as *L*. The *solid* noise-free curves represent the theoretical parameters convolved with the lamp. In *a*, the results of the analysis are shown for a monoexponential decay function; in *b*, the same decay data were analyzed as three exponential components. The plot of the weighted residuals (*center graphs*) and autocorrelation of the weighted residuals (*upper right inset*) are shown. The fluorescence decay parameters were: $\alpha = 0.59$, $\tau = 3.08$ ns, $\chi^2 = 17.29$ for a monoexponential decay (*a*) and $\alpha_1 = 0.20$, $\tau_1 = 1.28$ ns, $\alpha_2 = 0.22$, $\tau_2 = 3.41$ ns, $\alpha_3 = 0.02$, $\tau_3 = 7.57$ ns, $\chi^2 = 1.01$ for the three fluorescence decay components (*b*).

TABLE II

Time-resolved fluorescence intensity parameters of DARPP-32

The fluorescence intensity decay curves collected in the spectral range between 310 and 450 nm were analyzed by the global procedure and were used to produce the DAS presented in Fig. 6. $I\%_i$, are the relative intensity contributions of each decay component to the total emission spectrum, and have been calculated as normalized areas under the spectra ($\sum \alpha_i \cdot \tau_i$). The ratio between the relative intensities associated with the short and the long lifetime ($I\%_1/I\%_3$) were 1.198, 1.220, 1.192, and 0.395 for nonphosphorylated, PKA phosphorylated, CKII phosphorylated, and denatured DARPP-32, respectively. The intensity-weighted lifetime, τ_m, has been calculated at 350 mm as, $\sum(\alpha_i \cdot \tau_i^2)/\sum(\alpha_i \cdot \tau_i)$ (Chen *et al.*, 1991).

DARPP-32	τ_1	τ_2	τ_3	$I\%_1$	$I\%_2$	$I\%_3$	τ_m
		ns					*ns*
Nonphosphorylated	1.24	3.48	7.21	18.2	66.7	15.1	3.53
PKA phosphorylated	1.10	3.34	7.06	18.4	66.5	15.1	3.54
CKII phosphorylated	0.99	3.40	7.50	15.7	71.2	13.1	3.52
Nonphosphorylated, 8 M urea	0.62	3.26	7.05	10.3	63.8	25.9	3.76

DARPP-32 induced by ionic strength or site-specific phosphorylation during the excited state of tryptophan, nanosecond time-resolved DAS (Privat *et al.*, 1980; *et al.*, 1981; Knutson *et al.*, 1982; Neyroz *et al.*, 1987) were obtained. The DAS recovered from the nonphosphorylated, PKA-phosphorylated, CKII-phosphorylated, and denatured forms of DARPP-32 are shown in Fig. 6. In all native forms of DARPP-32, the relative intensity associated with the intermediate lifetime provided the highest contribution to the total emission intensity (67%), whereas the relative intensity associated with the short and long lifetimes contributed to a much lesser extent (18 and 15%, respectively). In the nonphosphorylated DARPP-32 (Fig. 6*A*), the spectral distributions of the intermediate and long lifetime components were similar to the steady-state emission spectrum, with a maximal emission intensity at 350 nm. On the other hand, the short lifetime component was slightly blue-shifted with respect to the other components and to the steady-state spectrum. No marked differences in the DAS were observed by changing the ionic strength of the medium (not shown) or after phosphorylation of DARPP-32 by PKA (Fig. 6*B*). Phosphorylation by CKII (Fig. 6*C*) did not change the spectral distribution of the lifetime components but slightly increased the relative contribution of the intermediate lifetime with respect to the other two components (see also Table II). Upon denaturation (Fig. 6*D*), the contribution of the short decay component became negligible, with a concomitant increase in the contribution of the long decay component, resulting in an increase of the mean lifetime (Table II). This observation is consistent with the fluorescence intensity changes observed in the steady-state emission

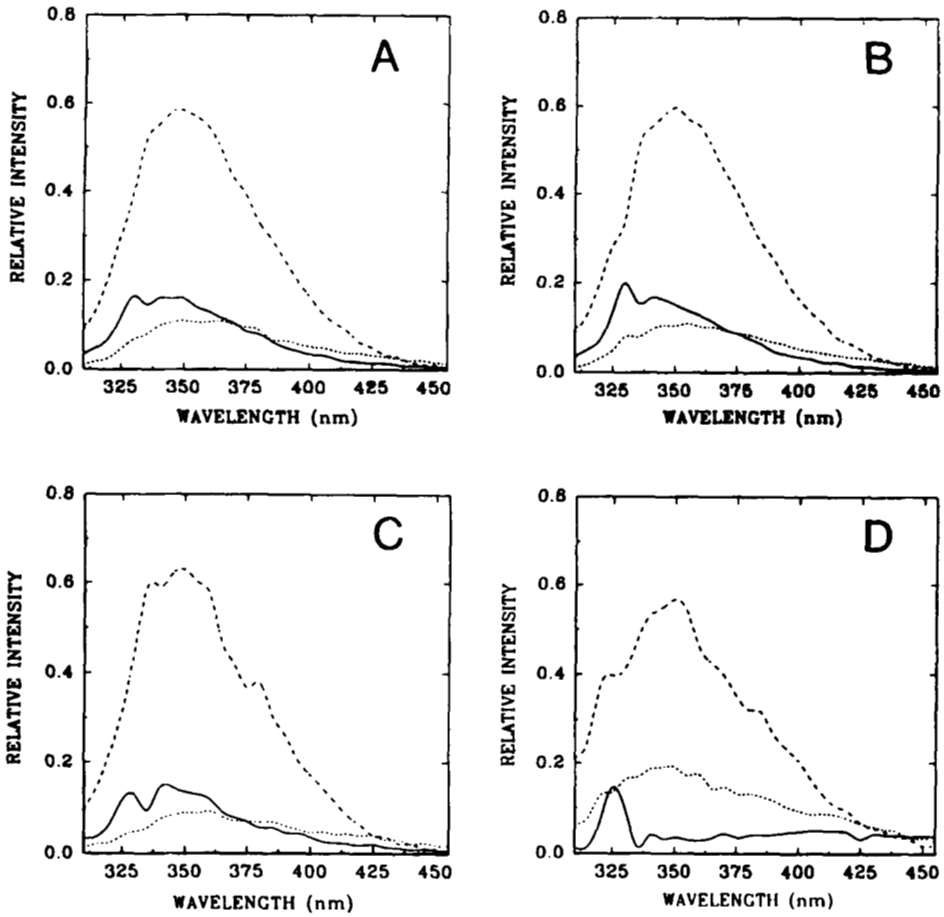

FIG. 6. **DAS of DARPP-32 in various states of phosphorylation.** The fluorescence decay of nonphosphorylated DARPP-32 (*panel A*), DARPP-32 phosphorylated on Thr^{34} by PKA (*panel B*), DARPP-32 phosphorylated on Ser^{45} and Ser^{102} by CKII (*panel C*), and nonphosphorylated DARPP-32 in 8 M urea (*panel D*) were measured at 22 °C in a buffer containing 10 mM Hepes, pH 7.4, 1 mM EDTA using an excitation wavelength of 295 nm. The data, expressed as relative intensity in each DAS, refer to the $\alpha_i \cdot \tau_i$ products. The spectra associated with the short, intermediate, and long lifetimes are represented with *solid*, *dashed*, and *dotted lines*, respectively. Decay curves were collected every 5 nm between 310 and 450 nm and the DAS were obtained by the global analysis method (see "Experimental Procedures"). Global reduced χ^2 ranged between 1.10 and 1.34.

spectrum recorded under denaturing conditions (see Fig. 3, *upper panel*). Although a short decay component was required to provide an adequate fit, it should be pointed out that the profile of the short lifetime DAS of denatured DARPP-32 is not a typical tryptophan distribution, in fact the largest area under the curve is in the region of the Raman peak. Considering that samples of equal protein concentration were used to obtain the DAS presented in Fig. 6, and thus comparable Raman contributions should underlie each DAS, we used the total area under the respective curves to calculate the intensities presented in Table II. This could cause a small underestimate of the mean lifetime calculated for the denatured DARPP-32.

The decay of both the intrinsic and the extrinsic emission anisotropy of DARPP-32 was resolved. In both cases, the fluorescence anisotropy decay was well described by a double exponential function with correlation times of 0.3–0.4 and 2–3 ns for tryptophan fluorescence and of 0.7–1.7 and 13–15 ns for lucifer yellow-cysteine fluorescence (Table III). The fast rotational movements resolved for the intrinsic emission anisotropy decay can be explained by the combination of independent flexibility of the COOH-terminal peptide chain and local mobility of the indole ring. On the other hand, the longer correlation times recovered from the anisotropy decay of lucifer yellow-labeled DARPP-32 indicate that the NH_2-terminal domain of the protein has limited rotational flexibility. Under denaturing conditions, the anisotropy decay of tryptophan fluorescence was best described by a single correlation time of approximately 0.9 ns and no improvement in the statistical parameters was obtained by fitting the data with an additional decay component. This rapid depolarization is typical for truly random coil structures. Phosphorylation of DARPP-32 either by PKA or CKII had relatively minor effect, inducing only a slight increase in the long correlation time of either tryptophan or lucifer yellow regions. A relatively high intrinsic variability was found in measuring the shortest correlation times of both tryptophan and lucifer yellow-cys-

TABLE III

Anisotropy decay parameters of DARPP-32

The decay of the emission anisotropy of DARPP-32 in various phosphorylation states and after urea-induced denaturation were measured at 22 °C as described under "Experimental Procedures." DARPP-32 was dissolved in a buffer containing 10 mM Hepes, pH 7.4, 1 mM EDTA at a concentration of 0.2 mg/ml. The experimental anisotropy decay data were analyzed as a sum of exponential terms ($r(t) = \sum \beta_i \cdot e^{-t/\Phi_i}$), where β_i represent the prexponential coefficients associated to each correlation time, ϕ_i and the time 0 anisotropy, r_o, is given by $\sum \beta_i$.

Tryptophan fluorescence					
DARPP-32	β_1	ϕ_1	β_2	ϕ_2	χ^2
		ns		*ns*	
Nonphosphorylated	0.06	2.10	0.08	0.46	0.10
PKA phosphorylated	0.07	3.20	0.10	0.36	1.02
CKII phosphorylated	0.06	2.70	0.20	0.28	1.37
Nonphosphorylated, 8 M urea	0.18	0.86			1.33
Lucifer yellow-cysteine fluorescence					
DARPP-32	β_1	ϕ_1	β_2	ϕ_2	χ^2
		ns		*ns*	
Nonphosphorylated	0.11	12.86	0.19	1.69	1.23
PKA phosphorylated	0.13	13.41	0.27	0.69	1.25
CKII phosphorylated	0.12	15.04	0.19	0.98	1.07

teine anisotropy decays, and no conclusions can be drawn from the changes in these components.

DISCUSSION

Protein phosphorylation is a reversible covalent modification of paramount importance by which extracellular signals can modulate intracellular events. Phosphorylation can modulate the functional properties by two major mechanisms: (i) the incorporation of a negatively charged phosphate group in a critical site of the molecule can modify its interactions with other molecules by local effects (*e.g.* loss of hydrogen bonds, steric hindrance, electrostatic interactions) without affecting the protein as a whole; (ii) the incorporation of the phosphate group can induce a conformational rearrangement involving the whole protein or a large part of it, which in turn is responsible for the change in the biological activity (Barford, 1991). In the present study, the intrinsic and extrinsic fluorescence of purified recombinant rat DARPP-32 has been characterized using steady-state and time-resolved techniques, with the purpose of better understanding the structure of the protein and the effects of microenvironment and site-specific phosphorylation on its biophysical properties. While steady-state fluorescence measurements can provide an intensity and time-averaged description of the probe environment, nanosecond time-resolved fluorescence spectroscopy is the tool of choice to monitor relevant biological events occurring in this time domain.

DARPP-32 is a cytosolic phosphoprotein that is highly concentrated in neurons receiving dopaminergic innervation and bearing D1 dopamine receptors (Hemmings *et al.*, 1987). The physiological properties of DARPP-32 have been mostly studied in rat, whereas the biochemical investigations have been carried out using bovine DARPP-32. To overcome this problem, we have expressed rat DARPP-32 in bacteria and used purified recombinant DARPP-32 for biochemical and photophysical investigations. The properties of the recombinant protein, including apparent M_r, phosphorylation by PKA and CKII, and inhibition of PP1c were indistinguishable from those of natural rat DARPP-32 and very similar to those of bovine DARPP-32.[2] The quasi-identical properties of natural and recombinant DARPP-32 are easily understandable since DARPP-32 appears to undergo no post-translational modification other than phosphorylation. In addition, its remarkable heat and acid resistance can account for the substantial preservation of biological activity and overall structure during the purification procedure. Hydrodynamic studies have revealed that DARPP-32, which has a low content of hydrophobic amino acids, exhibits an "unfolded" tertiary structure with a very elongated shape (Hemmings *et al.*, 1984b).

The CD data presented in this work revealed that DARPP-32 contains very little secondary structure, in partial contrast with the prediction based on the primary sequence (Williams *et al.*, 1986), but in substantial agreement with previous observations (Hemmings *et al.*, 1984b). In addition, the high accessibility of the intrinsic and extrinsic fluorophores to acrylamide and KI implied that the single tryptophan and cysteine residues, located in the NH_2- and COOH-terminal regions of the molecule, are completely exposed to the external aqueous medium. However, the presence of marked changes in both static and time-resolved intrinsic fluorescence parameters upon denaturation (see below) demonstrates that, under native conditions, DARPP-32 possesses features which differ from a completely unfolded protein. In fact, while the steady-state emission spectra of the extrinsically labeled DARPP-32 show only minor shifts upon denaturation, the intrinsic fluorescence exhibits a significant increase in intensity. From steady-state data such an effect can be generally assigned to the release of a quenching mechanism present in the native form. A characteristic charge distribution may be needed to sustain the native structure of DARPP-32 and can be related to its biological activity.

Nanosecond time-resolved dissection of the intrinsic fluorescence decay provides more detailed information on protein structure (Ross *et al.*, 1981; Knutson *et al.*, 1982; Beechem and Brand, 1985). Three major decay constants were recovered from the analysis of the data of DARPP-32. The relative intensity associated with the three lifetimes (1, 3.4, and 7.3 ns) revealed the predominant contribution of the intermediate lifetime (60–70%) with a ratio between the relative intensities associated with the short and the long lifetimes of 1.2. The complex photophysics of tryptophan in proteins has been related to a number of different mechanisms including conformational heterogeneity (Szabo and Rayner, 1980; Petrich *et al.*, 1983; Beechem and Brand, 1985). It is worth noting that the three lifetimes we recovered for DARPP-32 stringently reproduce a common result obtained with several proteins and tryptophan compounds (Petrich *et al.*, 1983; Beechem and Brand, 1985; Benfenati *et al.*, 1990; Chen *et al.*, 1991). Attempts have been made to correlate lifetime components with the existence of rotamer populations (Szabo and Rayner, 1980), their distribution, and their stability in the excited-state. Recently, Dahms *et al.* (1993) have provided new evidence for this model; they showed that in a protein crystal of *erabutoxin b* the proportion of each decay time is dependent on the orientation of the crystal. In general, for proteins in solution, multiexponential decays are explained on the basis of the presence of conformers, each with different fluorescence lifetimes. According to this representation, our results show that, in the native condition, a significant concentration of DARPP-32 exists in a conformational state (conformer) where the indole ring is quenched. Upon denaturation by 8 M urea, we found that the preexponential term of the long lifetime, α_3, increased in the absence of significant changes in the associated decay constant (Table II). This evidence confirms the possible release of a static quenching which depletes, under native conditions, the long lifetime conformer. This effect is clearly shown by the comparison of the DAS of *panels A–C* with the DAS of *panel D* in Fig. 6. The static quenching may result from negative charges in the proximity of the tryptophan residue. The primary sequence of rat DARPP-32 contains 3 glutamate residues in the immediate vicinity of Trp^{163} (at positions 160, 164, and 171). It is tempting to assign the long lifetime conformer to a conformation where glutamate residues can form dark complexes with Trp^{163}.

Unlike denaturation, the parameters of DARPP-32 transient fluorescence were not significantly affected by either salt concentrations or phosphorylation by PKA. Phosphorylation by CKII slightly increased the contribution of the intermediate lifetime component with a simultaneous decrease in the contribution of the long lifetime component. Since these changes are opposite with respect to those observed upon denaturation, they suggest that the CKII-phosphorylated form of DARPP-32 assumes a more ordered structure. The DAS report only on the local environment of tryptophan, hence we cannot rule out significant conformational changes in other domains. However, the absence of major changes on the tryptophan photophysics demonstrates that the microenvironment of the single tryptophan residue in the COOH-terminal region is little affected by post-translational modifications of Thr^{34}, Ser^{45}, and Ser^{102} residues.

The steady-state and time-resolved anisotropy revealed the

presence of a differential mobility/flexibility of the NH_2- and COOH-terminal parts of the molecule in the native state (with the NH_2-terminal region considerably more rigid than the COOH-terminal region) and of an increased overall molecular motion upon denaturation. In fact, the long correlation times recovered for lucifer yellow, with the different forms of native DARPP-32, suggest the existence of a folded, rigid environment, surrounding Cys^{72}. Thus, we postulate the existence of two distinct protein domains which may play an important role in modulating the interaction of DARPP-32 with PP1c. Phosphorylation by PKA or CKII did not grossly alter the structural configuration of either the NH_2- or the COOH-terminal regions of DARPP-32.

Structural changes associated with phosphorylation have been reported for several proteins, including glycogen phosphorylase (Sprang *et al.*, 1988; Johnson, 1992) and synapsin I (Benfenati *et al.*, 1990). Phosphorylation of Ser^{14} of glycogen phosphorylase affects the tertiary structure of the subunit and the quaternary structure of the holoenzyme; phosphorylation of Ser^{566} and Ser^{603} in the nerve terminal phosphoprotein synapsin I induces a major conformational change of the molecule which decreases its interactions with actin filaments and with the membrane of synaptic vesicles (Valtorta *et al.*, 1992). On the other hand, in the case of isocitrate dehydrogenase, phosphorylation of Ser^{113} inhibits enzyme activity by directly affecting the interaction of the substrate with the active site in the absence of long-range conformational changes (Hurley *et al.*, 1990a, 1990b).

The lack of gross conformational change upon phosphorylation of DARPP-32 on Thr^{34} by PKA contrasts with the potent activation of the PP1c inhibitory activity. This contrast suggests that it is the incorporation of a negatively charged phosphate group in a strongly positive region (with 4 arginines in a row) that has a direct effect on the interaction of DARPP-32 with PP1c. Kinetic studies had suggested that DARPP-32, as well as inhibitor 1, interact with PP1c at two sites, one of which includes the phosphorylated threonine which presumably blocks the phosphatase active site (Foulkes *et al.*, 1983; Hemmings *et al.*, 1984a, 1990). Such a local effect of Thr^{34} phosphorylation is in perfect agreement with the observation that short peptides encompassing the phosphorylated threonine (residues 9–38) inhibit PP1c efficiently (~20% of the activity of the holoprotein) (Hemmings *et al.*, 1990).

The interaction between DARPP-32 and PKA and its modulation by CKII phosphorylation seem to be more complex. Short peptides encompassing the PKA phosphorylation site of DARPP-32 or inhibitor 1 display poor phosphorylation kinetics as compared to the respective holoproteins (Hemmings *et al.*, 1984c, 1990; Foulkes *et al.*, 1983). The difference between peptides and holoprotein is less pronounced in the case of cGMP-dependent protein kinase which phosphorylates the same threonine as PKA (Hemmings *et al.*, 1984c, 1990). Interestingly phosphorylation of DARPP-32 by CKII improves its phosphorylation by PKA but not by cGMP-dependent protein kinase (Girault *et al.*, 1989). It is noteworthy that time-resolved fluorescence measurements indicate that phosphorylation by CKII has some influence on conformation of the protein. It will be interesting to determine whether the 12 residues that are conserved between inhibitor 1 and DARPP-32 and which are located between positions 75 and 117 play a role in the overall structural organization of these proteins and their interactions with PKA.

In conclusion, the available data suggest that DARPP-32 has a partially unfolded tertiary structure which does not undergo major conformational transitions after phosphorylation on specific sites by PKA or CKII. In this respect, the mechanism of activation of the phosphatase inhibitory activity by PKA phosphorylation seems to resemble more that of isocitrate dehydrogenase than those of either glycogen phosphorylase or synapsin I.

Acknowledgments—The technical assistance of Denise Porter in running the laser instrumentation is gratefully acknowledged. We are also grateful to Drs. L. Masotti, F. Valtorta, and N. Rosato for helpful discussions and critical reading of the manuscript.

REFERENCES

Aitken, A., Bilham, T., and Cohen, P. (1982) *Eur. J. Biochem.* **126,** 235–246
Ameloot, M., Hendrickx, H., Herreman, W., Pottel, H., Van Cauwelaert, F., and Van Der Meer, W. (1984) *Biophys. J.* **46,** 525–539
Azumi, T., and McGynn, S. P. (1962) *J. Chem. Phys.* **37,** 2413–2420
Badea, M. G., and Brand, L. (1979) *Methods Enzymol.* **61,** 378–425
Barford, D. (1991) *Biochim. Biophys. Acta* **1133,** 55–62
Beechem, J. M., and Brand, L. (1985) *Annu. Rev. Biochem.* **54,** 43–71
Beechem, J. M., Ameloot, M., and Brand, L. (1985) *Anal. Instr.* **14,** 379–402
Benfenati, F., Neyroz, P., Bähler, M., Masotti, L., and Greengard, P. (1990) *J. Biol. Chem.* **265,** 12584–12595
Bevington, P. R. (1969) *Data Reduction and Error Analysis for the Physical Science*, McGraw-Hill Inc., New York
Birks, J. B. (1970) *Photophysics of Aromatic Molecules*, John Wiley & Sons, New York
Chen, R. F., Knutson, J. R., Ziffer, H., and Porter, D. (1991) *Biochemistry* **30,** 5184–5195
Cross, A. J., and Fleming, G. R. (1984) *Biophys. J.* **46,** 45–56
Dahms, T. E. S., Willis, K. J., and Szabo, A. G. (1993) *Biophys. J.* **64,** A55
Dale, R. E., Chen, L. A., and Brand, L. (1977) *J. Biol. Chem.* **252,** 7500–7510
Eftink, M. R., and Ghiron, C. A. (1976) *Biochemistry* **15,** 672–680
Ehrlich, M. E., Kurihara, T., and Greengard, P. (1990) *J. Mol. Neurosci.* **2,** 1–10
Elbrecht, A., DiRenzo, J., Smith, R. G., and Shenolikar, S. (1990) *J. Biol. Chem.* **265,** 13415–13418
Foulkes, J. G., Strada, S. J., Henderson, P. J., and Cohen, P. (1983) *Eur. J. Biochem.* **132,** 309–313
Gilbert, C. W. (1983) in *Time-resolved Fluorescence Spectroscopy in Biochemistry and Biology* (Cundall, R. B., and Dale, R. E., eds) pp. 605–607, Plenum Press, New York
Girault, J.-A., Hemmings, H. C., Jr., Williams, K. R., Nairn, A. C., and Greengard, P. (1989) *J. Biol. Chem.* **264,** 21748–21759
Greenfield, N., and Fassman, G. D. (1969) *Biochemistry* **8,** 4108–4116
Grinvald, A., and Steinberg, I. Z. (1974) *Anal. Biochem.* **59,** 583–598
Halpain, S., Girault, J.-A., and Greengard, P. (1990) *Nature* **343,** 369–372
Hathaway, G. M., and Traugh, J. A. (1983) *Methods Enzymol.* **99,** 317–331
Haugland, R. P. (1992) *Handbook of Fluorescent Probes and Research Chemicals*, Molecular Probes Inc., Eugene, OR
Hemmings, H. C., Jr., Greengard, P., Tung, H. Y. L., and Cohen, P. (1984a) *Nature* **310,** 503–505
Hemmings, H. C., Jr., Nairn, A. C., Aswad, D. W., and Greengard, P. (1984b) *J. Neurosci.* **4,** 99–110
Hemmings, H. C., Jr., Nairn, A. C., and Greengard, P. (1984c) *J. Biol. Chem.* **259,** 14491–14497
Hemmings, H. C., Jr., Williams, K. R., Konigsberg, W. H., and Greengard, P. (1984d) *J. Biol. Chem.* **259,** 14486–14490
Hemmings, H. C., Jr., Walaas, S. I., Ouimet, C. C., and Greengard, P. (1987) *Trends Neurosci.* **10,** 377–383
Hemmings, H. C., Jr., Nairn, A. C., Elliott, J. I., and Greengard, P. (1990) *J. Biol. Chem.* **265,** 20369–20376
Hemmings, H. C., Jr., Girault, J.-A., Nairn, A. C., Bertuzzi, G., and Greengard, P. (1992) *J. Neurochem.* **59,** 1053–1061
Huang, F. L., and Glinsman, W. H. (1976) *Eur. J. Biochem.* **70,** 419–426
Hurley, J. H., Dean, A. M., Thorsness, P. E., Koshland, D. E., and Stroud, R. M. (1990a) *J. Biol. Chem.* **265,** 3599–3602
Hurley, J. H., Dean, A. M., Sohl, J. L., Koshland, D. E., and Stroud, R. M. (1990b) *Science* **240,** 1012–1016
Ingebritsen, T. S., and Cohen, P. (1983) *Eur. J. Biochem.* **132,** 255–261
Johnson, M. L. (1983) *Biophys. J.* **44,** 101–106
Johnson, M. L. (1992) *FASEB J.* **6,** 2274–2282
Kaczmarek, L. K., Jennings, K. R., Strumwasser, F., Nairn, A. C., Wilson, F. D., and Greengard, P. (1980) *Proc. Natl. Acad. Sci. U. S. A.* **77,** 7487–7491
King, M. M., Huang, C. Y., Chock, P. B., Nairn, A. C., Hemmings, H. C., Jr., Chan, K. F., and Greengard, P. (1984) *J. Biol. Chem.* **259,** 8080–8083
Knight, A. E. W., and Selinger, B. K. (1971) *Spectrochim. Acta Part A Mol. Spectrosc.* **27,** 1223–1234
Knutson, J. R., Walbridge, D. G., and Brand, L. (1982) *Biochemistry* **21,** 4671–4679
Knutson, J. R., Beechem, J. M., and Brand, L. (1983) *Chem. Phys. Lett.* **102,** 501–507
Kurihara, T., Lewis, R. M., Eisler, J., and Greengard, P. (1988) *J. Neurosci.* **8,** 508–517
Laemmli, U. K. (1970) *Nature* **227,** 680–685
Neyroz, P., Brand, L., and Roseman, S. (1987) *J. Biol. Chem.* **262,** 15900–15907
O'Connor, D. V., and Philips, D. (1984) *Time-correlated Single Photon Counting*, Academic Press, New York
Paoletti, J., and LePecq, J. B. (1969) *Anal. Biochem.* **31,** 33–41
Parker, C. A. (1968) *Photoluminescence of Solutions*, pp. 220–222, Elsevier Science Publishers, New York
Petrich, J. W., Chang, M. C., McDonald, D. B., and Fleming, G. R. (1983) *J. Am. Chem. Soc.* **105,** 3824
Prendergast, F. G., Meyer, M., Carlson, G. L., Iida, S., and Potter, J. D. (1983) *J. Biol. Chem.* **258,** 7541–7544
Privat, J. P., Wahl, P., Auchet, J. C., and Pain, R. H. (1980) *Biophys. Chem.* **11,** 239–248

Rosenberg, A. H., Lade, B. N., Chui, D.-S., Lin, S.-W., Dunn, J. J., and Studier, F. W. (1987) *Gene (Amst.)* **56,** 125–135
Ross, J. B. A., Schmidt, C. J., and Brand, L. (1981) *Biochemistry* **20,** 4369–4377
Smith, P. K., Krohn, R. I., Hermanson, G. T., Mallia, A. K., Gartner, F. H., Provenzano, M. D., Fujimoto, E. K., Goeke, N. M., Olson, B. J., and Klenk, D. C. (1985) *Anal. Biochem.* **150,** 76–85
Sprang, S. R., Acharya, K. R., Goldsmith, E. J., Stuart, D. I., Varvill, K., Fletterick, R. J., Madsen, N. B., and Johnson, L. N. (1988) *Nature* **336,** 215–221
Szabo, A. G., and Ranier, D. M. (1980) *J. Am. Chem. Soc.* **102,** 554
Tao, T. (1969) *Biopolymers* **8,** 609–632
Valtorta, F., Benfenati, F., and Greengard, P. (1992) *J. Biol. Chem.* **267,** 7195–7198
Wahl, P. (1969) *Biochim. Biophys. Acta* **175,** 55–64
Wahl, P., Auchet, J. C., and Donzel, B. (1974) *Rev. Sci. Instrum.* **45,** 28–32
Ware, R. W. (1972) in *Creation and Detection of the Excited State* (Lamola, A., ed) Vol. 1, Part A, pp. 213–302, Marcel Dekkar Inc., New York
Williams, K. R., Hemmings, H. C., Jr., LoPresti, M. B., Konigsberg, W. H., and Greengard, P. (1986) *J. Biol. Chem.* **261,** 1890–1903
Yguerabide, J. (1972) *Methods Enzymol.* **26,** 498–578